



**HAL**  
open science

## Polysialic acid glycomimetic promotes functional recovery and plasticity after spinal cord injury in mice

A. Mehanna, I. Jakovcevski, A. Acar, M. Xiao, G. Loers, G. Rougon, A. Irintchev, M. Schachner

### ► To cite this version:

A. Mehanna, I. Jakovcevski, A. Acar, M. Xiao, G. Loers, et al.. Polysialic acid glycomimetic promotes functional recovery and plasticity after spinal cord injury in mice. *Molecular Therapy*, 2010, 18 (1), pp.34-43. 10.1038/mt.2009.235 . hal-00555165

**HAL Id: hal-00555165**

**<https://hal.science/hal-00555165v1>**

Submitted on 9 Nov 2023

**HAL** is a multi-disciplinary open access archive for the deposit and dissemination of scientific research documents, whether they are published or not. The documents may come from teaching and research institutions in France or abroad, or from public or private research centers.

L'archive ouverte pluridisciplinaire **HAL**, est destinée au dépôt et à la diffusion de documents scientifiques de niveau recherche, publiés ou non, émanant des établissements d'enseignement et de recherche français ou étrangers, des laboratoires publics ou privés.

Copyright

# Polysialic Acid Glycomimetic Promotes Functional Recovery and Plasticity After Spinal Cord Injury in Mice

Ali Mehanna<sup>1</sup>, Igor Jakovcevski<sup>1</sup>, Ayşe Acar<sup>1</sup>, Meifang Xiao<sup>1</sup>, Gabriele Loers<sup>1</sup>, Geneviève Rougon<sup>2</sup>, Andrey Irintchev<sup>1,3</sup> and Melitta Schachner<sup>1,4,5</sup>

<sup>1</sup>Zentrum für Molekulare Neurobiologie, Universität Hamburg, Hamburg, Germany; <sup>2</sup>Institut de Biologie du Développement de Marseille-Luminy (IBDML), Université de la Méditerranée, CNRS 6216, Parc Scientifique de Luminy, Marseille, France; <sup>3</sup>Department of Otorhinolaryngology, Friedrich-Schiller-University Jena, Jena, Germany; <sup>4</sup>W.M. Keck Center for Collaborative Neuroscience and Department of Cell Biology and Neuroscience, Rutgers University, Piscataway, New Jersey, USA; <sup>5</sup>Center for Neuroscience, Shantou University Medical College, Shantou, China

Regeneration after injury of the central nervous system is poor due to the abundance of molecules inhibiting axonal growth. Here we pursued to promote regeneration after thoracic spinal cord injury in young adult C57BL/6J mice using peptides which functionally mimic polysialic acid (PSA) and human natural killer cell-1 (HNK-1) glycan, carbohydrate epitopes known to promote neurite outgrowth *in vitro*. Subdural infusions were performed with an osmotic pump, over 2 weeks. When applied immediately after injury, the PSA mimetic and the combination of PSA and HNK-1 mimetics, but not the HNK-1 mimetic alone, improved functional recovery as assessed by locomotor rating and video-based motion analysis over a 6-week observation period. Better outcome in PSA mimetic-treated mice was associated with higher, as compared with control mice, numbers of cholinergic and glutamatergic terminals and monaminergic axons in the lumbar spinal cord, and better axonal myelination proximal to the injury site. In contrast to immediate post-traumatic application, the PSA mimetic treatment was ineffective when initiated 3 weeks after spinal cord injury. Our data suggest that PSA mimetic peptides can be efficient therapeutic tools improving, by augmenting plasticity, functional recovery when applied during the acute phase of spinal cord injury.

Received 12 May 2009; accepted 14 September 2009; published online 13 October 2009. doi:10.1038/mt.2009.235

## INTRODUCTION

Severed axons in the adult mammalian central nervous system do not regenerate.<sup>1</sup> Regeneration failure is attributed to inhibitory molecules generating a nonpermissive environment for axonal regrowth and reshuffling of synaptic connections<sup>2–4</sup> and to a low intrinsic capacity of neurons for axonal regrowth.<sup>5</sup> Overcoming the inhibitory cues and enhancing the conducive ones is an important

aim in promoting functional recovery after spinal cord lesion in adult mammals including humans.

An emerging approach to improve regeneration is the use of carbohydrates or their mimetic peptides. Such carbohydrates, like polysialic acid (PSA) and the human natural killer cell-1 (HNK-1) cell carbohydrate are attached to cell adhesion and extracellular matrix molecules and finely tune cell interactions in the nervous system during development, regeneration and synaptic plasticity.<sup>6</sup> PSA, a unique glycan associated with the neural cell adhesion molecule (NCAM),<sup>7,8</sup> is expressed most prominently during development and is essential for neuronal and glial cell migration, outgrowth of axons, axonal branching, and fasciculation.<sup>9</sup> PSA is upregulated after various types of central and peripheral nervous system lesion,<sup>7</sup> and overexpression of PSA by lesion scar astrocytes or transplantation of PSA-overexpressing Schwann cells improves regeneration after spinal cord injury.<sup>10–12</sup> And, as recently shown, PSA glycomimetics improve functional recovery and remyelination after femoral nerve lesion in mice.<sup>13</sup>

The HNK-1 carbohydrate is carried by or binds to different neural recognition molecules among them the myelin-associated glycoprotein, several laminin isoforms, amphoterin, NCAM, L1, P0, and highly acidic glycolipids.<sup>6</sup> Interactions of the HNK-1 epitope with chondroitin sulfate proteoglycans enhance neuronal cell adhesion and neurite outgrowth<sup>14</sup> and HNK-1 glycomimetics<sup>15</sup> promote functional recovery after peripheral nerve injury in adult mice.<sup>16</sup>

In this study we examined whether PSA and HNK-1 mimetics, infused alone or in combination over 2 weeks by an osmotic pump, would improve the outcome of spinal cord compression injury in mice. We found beneficial effects when a PSA mimetic was applied alone or in combination with a HNK-1 mimetic, but no effect of HNK-1 mimetic alone when compared to control peptide (CON) treated mice. Importantly, the effect of the PSA mimetic was present when it was applied immediately after compression injury, *i.e.*, during the acute phase of injury, but not when infusion was initiated in the chronic phase, at 3 weeks after injury.

**Correspondence:** Melitta Schachner, Center for Neuroscience, Shantou University Medical College, Shantou, China.  
E-mail: Schachner@Biology.Rutgers.Edu

## RESULTS

## Delivery of peptides to the injured spinal cord

First, we analyzed the efficacy of peptide delivery to the injured spinal cord via an Alzet osmotic pump. As glycomimetics cannot be distinguished with antibodies from the endogenous epitopes which they mimic, we infused an exogenous protein fragment, human immunoglobulin Fc, which is not expressed in the mouse spinal cord. Two weeks after compression of the thoracic spinal cord and continuous infusion of 12.5  $\mu\text{g}/\text{ml}$  protein at the sacral level over this period, the Fc fragment was well detectable by

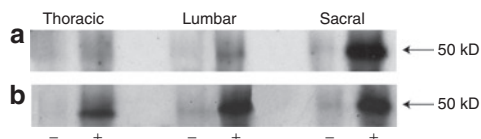


**Figure 1** Efficacy of protein application to the acutely injured mouse spinal cord. Western blot analysis of thoracic, lumbar, and sacral spinal cord tissue homogenates after pump application of PBS (-) or of a human Immunoglobulin G Fc fragment (+) into the cauda equina over a 2-week period. **(a)** Homogenates from spinal cords which received 12.5  $\mu\text{g}/\text{ml}$  Fc, and **(b)** homogenates from spinal cords which received 200  $\mu\text{g}/\text{ml}$  Fc. Note that a high concentration is necessary for efficient peptide delivery to the thoracic spinal cord where the lesion is performed. Forty  $\mu\text{g}$  of protein were loaded into each lane.

immunoblot analysis in the sacral segments of the spinal cord (**Figure 1a**). At the lumbar level, Fc protein was less detectable, and no Fc was detectable in the thoracic segments, *i.e.*, at the site of injury (**Figure 1a**). These observations indicated that high protein or peptide concentrations were necessary to create an efficient diffusion gradient for its remote delivery. Indeed, infusion of the Fc fragment at 200  $\mu\text{g}/\text{ml}$  resulted in a more homogeneous distribution of the protein in the caudo-rostral axis, with an efficient delivery up to the thoracic spinal cord (**Figure 1b**). Considering these results and aiming to deliver functionally most effective amounts of peptides to the site of injury, we applied the PSA and HNK-1 mimetics at 500  $\mu\text{g}/\text{ml}$ , the highest concentration at which the peptide solutions did not form precipitates, when kept at 37  $^{\circ}\text{C}$  under sterile conditions *in vitro* over a 2-week period during which the osmotic pumps deliver peptides *in vivo*.

## Improved motor recovery after immediate post-traumatic administration of a PSA mimetic

We designed four experimental groups in which either CON, PSA mimetic, HNK-1 mimetic, or combination of PSA plus HNK-1 mimetics were applied during the first 2 weeks after injury. Spinal cord compression caused severe locomotor disabilities in all mice, as assessed by the Basso Mouse Scale (BMS) scores<sup>17</sup> at 1 week after injury (**Figure 2a**). Between 1 and 6 weeks, the walking abilities

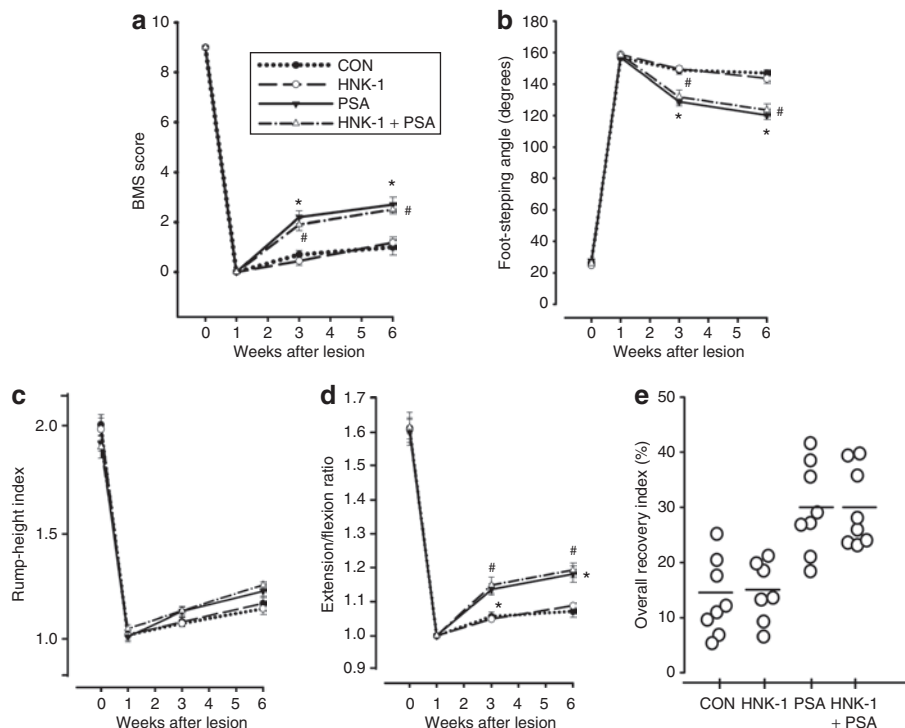


**Figure 2** Analysis of motor function. Time course and degree of recovery in mice treated with polysialic acid (PSA) mimetic, human natural killer cell-1 (HNK-1) mimetic, HNK-1 + PSA, and control peptide (CON) after acute spinal cord injury. Shown are mean values  $\pm$  SEM of **(a)** Basso Mouse Scale (BMS) scores, **(b)** foot-stepping angles, **(c)** rump-height indexes, and **(d)** extension-flexion ratios. Asterisks and hashes indicate values significantly different from the CON and HNK-1 group values at a given period ( $P < 0.05$ , one-way analysis of variance for repeated measurements with Tukey's post hoc test;  $n = 7-8$  mice per group), and **e** shows overall recovery indexes in individual mice at 6 weeks after injury. Horizontal lines in **e** indicate group mean values. The recovery index is an individual animal estimate calculated in percent as  $[(X_{7+n} - X_7) / (X_0 - X_7)] \times 100$ , where  $X_0$ ,  $X_7$ , and  $X_{7+n}$  are values prior to operation, 7 days after injury, and a time-point  $n$  days after the spinal cord injury, respectively. In simpler terms, this measure estimates gain of function after the first week ( $X_{7+n} - X_7$ ) as a fraction of the functional loss ( $X_0 - X_7$ ) induced by the operation. An overall recovery index is the mean of the recovery indexes calculated for the parameters shown in **a-d**.

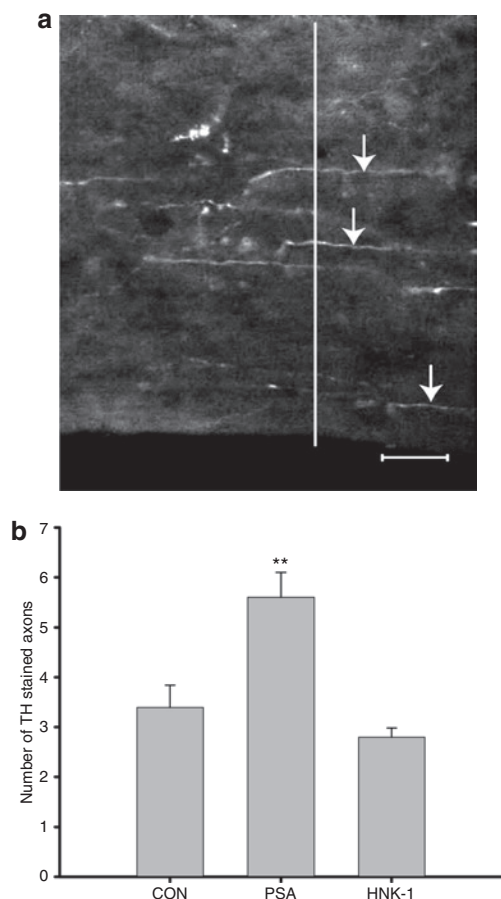


**Figure 3** Analysis of the monaminergic innervation of the lumbar spinal cord after treatment with control peptide (CON) and poly-sialic acid (PSA) or human natural killer cell-1 (HNK-1) mimetics of the acutely injured mouse spinal cord. **(a)** Representative image of tyrosine hydroxylase (TH) staining in the lumbar spinal cord 6 weeks after injury. **(b)** Mean numbers of TH<sup>+</sup> axons per section crossing an arbitrary border 250  $\mu$ m caudally from the lesion site (vertical line in **a**) 6 weeks after lesion (\*\* $P < 0.01$  compared with the CON and HNK-1 groups;  $N = 5$  mice per group; one-way analysis of variance with Tukey's post hoc test). Bar = 20  $\mu$ m.

improved more in mice which received PSA and PSA/HNK-1 mimetics than in mice treated with CON or HNK-1 mimetic (**Figure 2a**). In addition to the BMS, we analyzed the plantar stepping ability of the animals using our previously described parameter, the foot-stepping angle.<sup>18</sup> This analysis revealed, in agreement with the BMS, better recovery in the PSA and PSA/HNK-1 mimetic groups than in mice treated with HNK-1 mimetic or CON at both 3 and 6 weeks after injury (**Figure 2b**). We further evaluated more complex motor functions than plantar stepping.<sup>18</sup> Analysis of the rump-height index, a measure of the ability to support body weight during ground locomotion, showed similar, severe degree of disability at 1 week after injury and similar recovery thereafter in all experimental groups (**Figure 2c**). However, the ability of animals to perform voluntary movements without body weight support, estimated by the extension–flexion ratio, recovered significantly better with PSA and PSA/HNK-1 mimetic treatment than with CON or HNK-1 mimetic (**Figure 2d**). Finally, independent of treatment, numbers of correct steps made by the

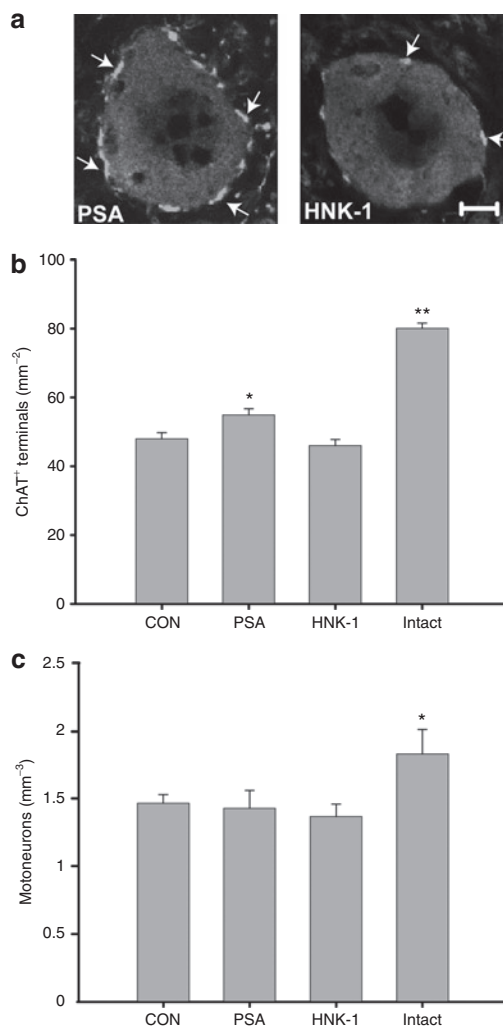


**Figure 4** Analysis of cholinergic terminals and motoneuron numbers in the lumbar spinal cord, i.e. caudal to the injury site, after treatment with control peptide (CON) and PSA or HNK-1 mimetics of the acutely injured mouse spinal cord. **(a)** Individual choline acetyltransferase (ChAT<sup>+</sup>) motoneurons in the lumbar spinal cord of mice treated with polysialic acid (PSA) or human natural killer cell-1 (HNK-1) mimetics (bar = 5  $\mu$ m). Arrows point to ChAT<sup>+</sup> perisomatic terminals. **(b)** Higher numbers of cholinergic synapses were found around motoneurons of mice treated with PSA glycomimetic compared to control and HNK-1 peptide 6 weeks after injury (\* $P < 0.05$ , one-way analysis of variance (ANOVA) with Tukey's post hoc test). The values for all groups of mice with spinal cord injury (CON, PSA, HNK-1) were significantly smaller than in uninjured (Intact) mice (\*\* $P < 0.05$ , one-way ANOVA with Tukey's post hoc test). Approximately 100 motoneurons were analyzed per group (five animals). **(c)** No difference among the groups with spinal cord injury was found for motoneuron density in the lumbar part of the spinal cord 6 weeks after injury. Interestingly, motoneuron density in the intact spinal cord is significantly higher compared with all other groups (\* $P < 0.05$ , one-way ANOVA with Tukey's post hoc test).

animals during inclined ladder climbing were reduced to almost 0 after 1 week of injury and did not significantly improve at 3 and 6 weeks (data not shown). We also calculated individual recovery indexes (RI) (degree of return of function, 100% indicating complete recovery) for each of the four parameters and mean of these RI per animal designated overall recovery index. At 6 weeks after injury, the overall RI of PSA and PSA/HNK-1 mimetic-treated

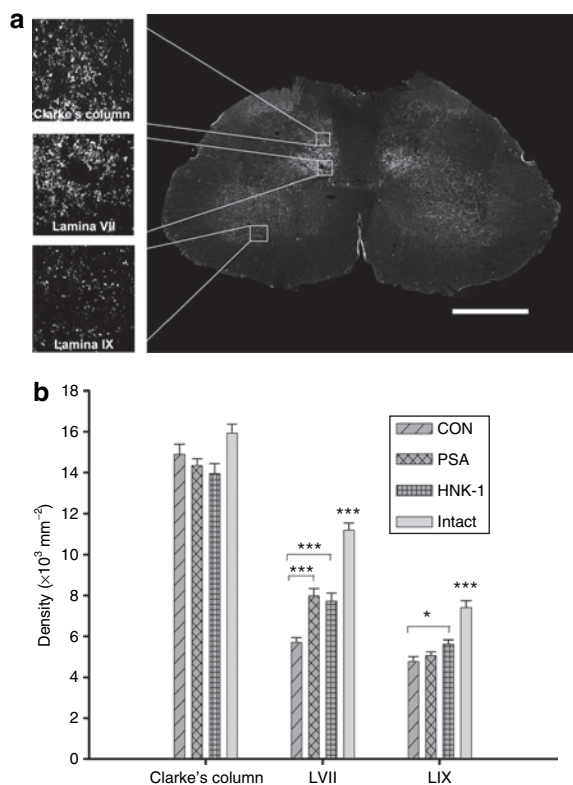


**Figure 5** Analysis of VGLUT1 terminal densities in the lumbar spinal cord 6 weeks after injury and treatment with control peptide (CON) and PSA or HNK-1 mimetics. **(a)** Representative image of a VGLUT1 stained spinal cord (bar = 200  $\mu\text{m}$ ). **(b)** Density (means  $\pm$  SEM) of VGLUT1<sup>+</sup> terminals in spinal cords of CON, polysialic acid (PSA), and human natural killer cell-1 (HNK-1) peptide treated spinal cord injured mice and uninjured mice (Intact), measured in three different areas: Clarke's column, lamina VII and lamina IX (see **a**). Compared with the CON group, more glutamatergic synapses were found in lamina VII in both PSA and HNK-1 treated mice, and in lamina IX after HNK-1 treatment. In the intact spinal cord, glutamatergic terminal density is significantly higher in Laminae VII and IX, but not in the Clarke's column, compared with all other groups ( $*P < 0.05$  and  $***P < 0.001$ , one-way analysis of variance with Tukey's post hoc test).  $N = 5$  animals per group.

mice were significantly higher than in mice treated with CON or HNK-1 mimetic (**Figure 4e**). In conclusion, these results show that treatment with the PSA mimetic, alone or in combination with the HNK-1 mimetic, but not HNK-1 mimetic alone, improves the functional outcome of compression spinal cord injury compared with the control treatment. Although this treatment does not restore walking after severe spinal cord injury, considerably improved stepping abilities and voluntary movements without body weight support are of clinical relevance.

Both the BMS scores and the numerical parameters used for our functional analysis strongly depend on the lesion severity.<sup>18,19</sup> We thus estimated lesion scar volume in control mice, as well as in mice treated with PSA and HNK-1 mimetics at 6 weeks after injury. The mean volume of the lesion scar was similar in all three groups of mice ( $0.14 \pm 0.01$ ,  $0.15 \pm 0.02$ , and  $0.15 \pm 0.02$  mm<sup>3</sup>, in phosphate-buffered saline (PBS), PSA and HNK-1 treated groups, respectively;  $P > 0.05$ , analysis of variance with Tukey's post hoc test). We conclude that enhanced functional recovery after PSA mimetic treatment is not related to attenuated tissue scarring.

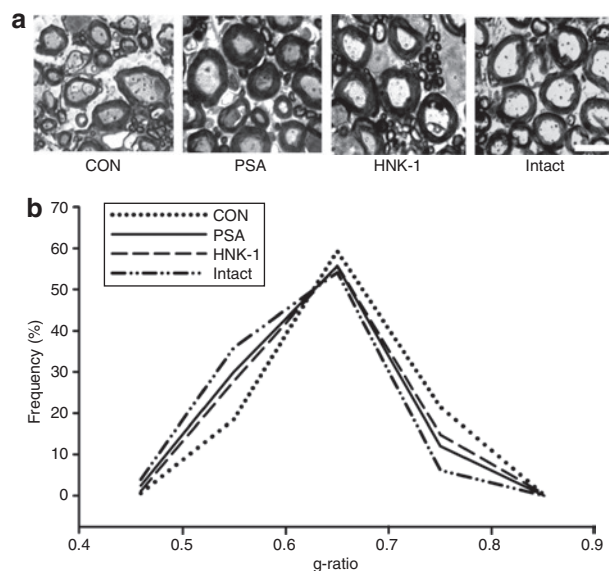


**Figure 6** Analysis of axonal myelination proximal to the spinal cord injury. **(a)** Representative images of axons from spinal cords of mice treated with control peptide (CON), polysialic acid (PSA) mimetic, human natural killer cell-1 (HNK-1) mimetic, as well as from intact mice are shown (bar = 3  $\mu\text{m}$ ). **(b)** Frequency distributions of g-ratios in the four groups. Animals treated with PSA and HNK-1 mimetics have significantly better myelination compared with CON as shown by the shift to lower g-ratio values ( $P < 0.05$ , Kolmogorov–Smirnov test). Five animals and ~500 axons were analyzed per group.

We also considered the possibility that the infused peptides might be immunogenic. To address this issue, we stained spinal cord sections from animals treated with PSA mimetic, HNK-1 mimetic or CON with antibodies against CD4 and CD8, markers of T-helper and T-cytotoxic lymphocytes, respectively. At 6 weeks after injury and initiation of the 2-week peptide infusion, we found only a few lymphocytes, often apparently located in blood vessels, per spinal cord section in all groups ( $9.0 \pm 0.7$ ,  $9.5 \pm 0.8$ , and  $8.7 \pm 0.8$  in CON, PSA mimetic and HNK-1 mimetic-treated mice, respectively,  $P > 0.05$ , one-way analysis of variance with Tukey's post hoc test). This finding indicates that the infused peptides do not cause inflammatory responses.

### Enhanced catecholaminergic, cholinergic, and glutamatergic innervation in the lumbar spinal cord after PSA treatment

Recovery of locomotor abilities after spinal cord injury depends on the extent of regrowth and/or sprouting of monoaminergic axons.<sup>20–22</sup> To assess whether improved motor functions in PSA mimetic-treated mice were related to enhanced monoaminergic innervation of the spinal cord caudal to the injury, we counted numbers of catecholaminergic tyrosine hydroxylase-positive axons projecting beyond an arbitrarily selected border 250  $\mu\text{m}$  caudally to the lesion site in spaced serial (250  $\mu\text{m}$  apart) parasagittal sections 6 weeks after the injury (**Figures 3a,b**). The mean number of tyrosine hydroxylase-positive axons per section in PSA mimetic-treated mice was significantly higher than in CON or HNK-1 mimetic-treated animals (**Figure 3b**). This observation indicates a more vigorous regenerative response, *i.e.*, axonal regrowth and/or

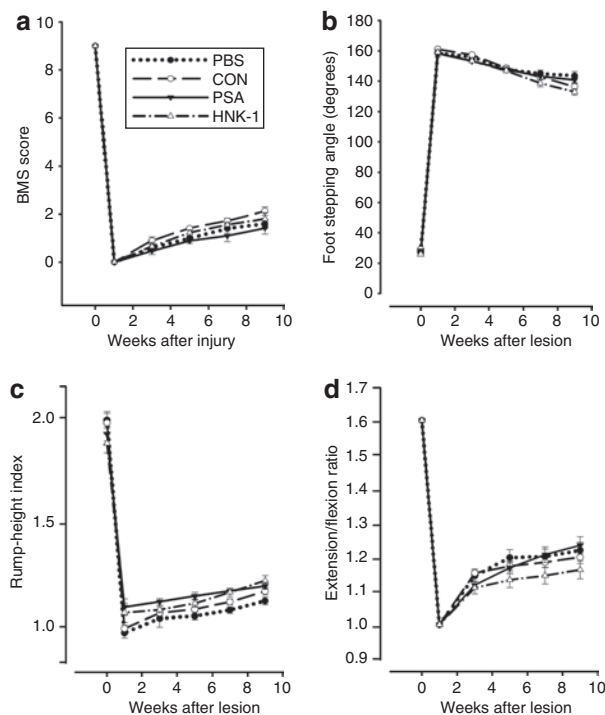


**Figure 7** Analysis of motor functions after glycomimetic application in chronically spinal cord injured mice. Time course and degree of recovery in mice in which a 2-week treatment with phosphate-buffered saline (PBS), control peptide (CON), human natural killer cell-1 (HNK-1), or polysialic acid (PSA) mimetics was initiated at 3 weeks after injury. Shown are mean  $\pm$  SEM values of (a) Basso Mouse Scale (BMS) scores, (b) foot-stepping angles, (c) rump-height indexes, and (d) extension–flexion ratios. No differences among the groups were found at any time point studied ( $P > 0.05$ , one-way analysis of variance for repeated measurements with Tukey's post hoc test;  $n = 10$  mice per group).

sprouting, of monoaminergic fibers in the injured spinal cord upon application of PSA mimetic which is in agreement with better recovery after PSA treatment.

We have previously reported, and confirmed here (Figure 4b), that the density of large perisomatic cholinergic choline acetyltransferase (ChAT<sup>+</sup>) boutons, known to form C-type synapses on motoneurons associated with muscarinic type 2 receptors<sup>23–25</sup> is strongly reduced in the lumbar spinal cord after thoracic spinal cord compression in mice.<sup>18,22</sup> Importantly, the locomotor performance assessed by the BMS score or the foot-stepping angle positively correlated with the number of these terminals 6 weeks after spinal cord injury.<sup>22</sup> We measured cholinergic synaptic coverage of motoneuron cell bodies in PSA mimetic, HNK-1 mimetic and CON treated animals (Figure 4a,b). Compared with CON, the number of ChAT<sup>+</sup> terminals was significantly increased (+15%) in PSA, but not in HNK-1 mimetic-treated mice (Figure 4b). We conclude that infusion of PSA mimetic partially prevents synaptic loss and/or promotes reestablishment of synaptic connections to lumbar motoneurons after injury, thus positively influencing recovery of motor functions.

To evaluate whether the glycomimetics used in this study influence cell survival, we analyzed motoneuron densities in the lumbar spinal cord and found no differences between mice treated with PSA mimetic, HNK-1 mimetic or CON (Figure 4c).

However there was a significant reduction of motoneuron density in all groups compared with the intact spinal cord, indicating motoneuron loss or reduction of ChAT expression after injury. Also no effect of PSA or HNK-1 mimetics, as compared with control treatment, on motoneuron soma size was found (data not shown). These findings indicate that different outcomes of spinal cord injury in PSA and HNK-1 mimetic-treated mice cannot be related to different, positive or adverse, effects on motoneurons.

The degree of locomotor recovery after spinal cord injury is largely determined by preservation and functionality of primary afferent inputs.<sup>26,27</sup> We were, therefore, interested whether spinal cord connectivity is altered in mimetic-treated mice compared with controls at 6 weeks after injury. We analyzed VGLUT1<sup>+</sup> synaptic terminals, which are derived from medium- to large-sized neurons in the dorsal root ganglia and convey mechano- and proprioceptive information to the spinal cord.<sup>28</sup> We selected three areas for analysis in which VGLUT1<sup>+</sup> terminal densities were prominent: Clarke's column which receives proprioceptive information, an adjacent part of lamina VII, a lamina in the spinal cord containing, among other neurons, last-order interneurons, *i.e.*, innervating motoneurons, and the motoneuron region, lamina IX, where proprio- and mechanoreceptors form contacts predominantly on motoneuron dendrites (Figure 5a). In mice treated with control, PSA and HNK-1 peptides there was no difference in density of VGLUT1<sup>+</sup> terminals in Clarke's column, but in lamina VII the density was increased after treatment with both PSA and HNK-1 mimicking peptides compared with the control animals (Figure 5b). Additionally, after treatment with HNK-1 peptide there was a small, but significant increase in the density of VGLUT1<sup>+</sup> terminals in lamina IX, around motoneurons, compared with both control and PSA mimetic-treated animals. This treatment-related difference indicates that treatment with glycomimetics results in an area-specific increase in afferent inputs to the injured spinal cord. Interestingly, analysis of glutamatergic terminal density in intact spinal cord show that spinal cord injury leads to a significant loss of glutamatergic synapses in laminae VII and IX but not in the Clarke's column (Figure 5b).

### PSA treatment enhances axonal myelination rostral to the site of injury

PSA plays an important role in primary myelination and remyelination.<sup>11,29,30</sup> Also the PSA mimetic used here has a beneficial effect on axonal remyelination as recently shown in a peripheral nerve lesion model in mice.<sup>13</sup> As spinal cord injury is associated with considerable demyelination, we hypothesized that the beneficial effect of the PSA mimetic on motor recovery after spinal cord injury could be mediated by promotion of central nervous system myelination. We stained serial horizontal sections of spinal cords treated with PSA mimetic, HNK-1 mimetic and CON with luxol fast blue. Analysis of the areas occupied by luxol fast blue-positive structures within the borders 5 mm rostral to 5 mm caudal from the lesion site was similar in the three experimental groups (data not shown), indicating that superior functional recovery was not related to better remyelination or reduced demyelination in the PSA mimetic-treated group. In accordance with this notion, a more refined analysis of the degree of axonal myelination by measuring g-ratios (axon-to-fiber

diameters of individual axons) in semi-thin sections from the ventral white matter in the lumbar spinal cord revealed no differences among the animal groups (data not shown). However, the PSA mimetic showed a considerable effect on the relative degree of myelination rostral to the injury site. Although the g-ratios in CON treated mice were increased (indicating worse myelination) compared with uninjured mice, the frequency distribution of the g-ratios were near-normal in PSA mimetic and, interestingly, also in HNK-1 mimetic-treated animals (Figure 6). The overall results do not allow the conclusion that the PSA mimetic has a direct effect on axonal myelination. The improvement observed most distally to the site of PSA mimetic application, *i.e.*, rostral to the injury site at mid-thoracic level, might be a secondary phenomenon related to better preservation and/or regeneration of axons above the lesion site, which would then be more prone to myelination. Nevertheless, better axonal myelination may contribute to better functional recovery after PSA mimetic application.

### The therapeutic time window of the PSA mimetic is limited to acute spinal cord injury

Considering that application of PSA mimetic immediately after injury over a period of 2 weeks leads to enhanced recovery of locomotor function, we tested whether a similar beneficial outcome of the 2-week treatment could be achieved when PSA application was initiated 3 weeks after spinal cord injury. At this time point the cellular consequences of injury, such as scar formation, and most of the spontaneous locomotor recovery in C57BL/6J mice have been reached,<sup>17,18,22</sup> but in the lumbar spinal cord caudal from the lesion site some tissue remodeling is still active.<sup>31</sup> No differences among the groups were found for any of the parameters measured during the 9-week observation period after injury (Figures 7a–d). This finding suggests that PSA mimetic treatment is effective only when initiated during the acute phase of spinal cord injury.

## DISCUSSION

This study demonstrates the feasibility, safety and efficacy of a PSA glycomimetic as a therapeutic means for spinal cord injury in an animal model. We also show that, the therapeutic time window of this treatment is limited to the acute post-traumatic phase. The positive functional effects of the mimetic appear to be achieved by endorsement of plasticity in the spinal cord.

### Improved functional outcome after PSA mimetic treatment

Previous studies have shown that exogenous PSA is beneficial for spinal cord regeneration. Viral-mediated overexpression of PSA enhances the regrowth of severed corticospinal and sensory axons.<sup>10,12</sup> Grafting of Schwann cells engineered to overexpress PSA in the injured spinal cord promotes functional recovery.<sup>11</sup> The use of peptides that mimic PSA, as evaluated in this study, offers a more direct, clinically feasible opportunity than gene- and cell-based approaches. Large amounts of peptide can readily be synthesized and subdural chronic application in humans is practicable. The application of peptides appears safe as no chronic T cell responses were observed and motoneuron numbers, tissue scarring and demyelination were not negatively affected.

PSA glycomimetic application improved two aspects of motor performance in injured mice: walking and voluntary movements without body weight support. The latter finding is of special interest from a clinical point of view. Walking is controlled in a highly automated way by the spinal cord via central pattern generators and local reflex pathways. After injury, even with a complete transection, high levels of functional recovery of stepping can be achieved in adult mammals by training the autonomic functions of the spinal cord.<sup>32,33</sup> In contrast, functionally meaningful voluntary movements, for example target-oriented limb movements, are primarily under supraspinal control and the extent of trainability of the neuronal circuitries controlling such motor skills remains to be further exploited.<sup>34,35</sup>

At the cellular level, we found several effects of the PSA mimetic which can explain the enhanced functional outcome. As compared with CON, more perisomatic cholinergic terminals were preserved on lumbar motoneurons, higher numbers of glutamatergic terminals were present in lamina VII of the spinal gray matter, and the monoaminergic innervation of the lumbar spinal cord was enhanced after PSA glycomimetic treatment. These phenomena can be interpreted as signs of enhanced axonal sprouting and synaptic maintenance/reshuffling, *i.e.*, augmented structural plasticity in the injured spinal cord. This notion is consistent with the view that plasticity of neuronal circuitries determines the outcome of spinal cord injury<sup>32,36</sup> and with the plasticity-promoting properties of PSA.<sup>6,8</sup> PSA is a cell-surface glycan with a large hydration volume that modulates the distance, and thus contacts between cells. This regulation in a “slippery eel,” nonreceptor fashion, influences different developmental mechanisms including growth and targeting of axons. Endogenous PSA is carried by the membrane-associated and soluble forms of the NCAM,<sup>37,38</sup> as well as by neuropilin-2 (ref. 39) which limits its actions to cells expressing these molecules. In contrast, application of a soluble exogenous PSA, or its functional mimetic, is not prone to this limitation and more widespread effects can be expected. In addition to a receptor independent mode of action, the PSA mimetic may be effective by influencing its endogenous carrier, NCAM. PSA is a positive modulator of NCAM function since its removal from NCAM is associated with an inhibition of NCAM functions like enhancement of long-term potentiation, axonal growth, synaptic plasticity, and learning and memory.<sup>40–42</sup> Interactions of the PSA mimetic with PSA-NCAM may stimulate regeneration-promoting NCAM functions and/or disrupt inhibitory PSA-NCAM/receptor interactions. In support of this notion is our recent finding that the PSA mimetic influences elongation of Schwann cell processes via an NCAM/fibroblast growth factor receptor-mediated mechanism.<sup>13</sup>

### Lack of functional effects after HNK-1 glycomimetic application

We have previously observed that both the HNK-1 and the PSA mimetics used in this study efficiently promote recovery of function after peripheral nerve injury.<sup>13,16</sup> In light of these observations and the positive effects of the PSA mimetic reported here, the lack of an effect of the HNK-1 mimetic on locomotor function was unexpected. HNK-1, similar to PSA, promotes synaptic plasticity in the central nervous system<sup>6,43</sup> and here we found evidence

for a positive influence of the HNK-1 mimetic on glutamatergic synapses. Similar to the PSA mimetic, the HNK-1 mimetic also improved myelination in the proximal part of the lesioned spinal cord. However, other important PSA mimetic effects like enhancement of the monoaminergic innervation in the lumbar spinal cord and the cholinergic synaptic coverage of motoneurons, previously found to be associated with better recovery,<sup>18,22</sup> were not observed. Therefore, we must assume that the inefficacy of the HNK-1 mimetic, as revealed by our functional tests, is related to its inability to influence the cholinergic and monoaminergic axons caudal to the lesion site. In addition to this simple notion, however, we have to consider that the HNK-1 epitope is carried by a larger number, as compared with PSA, of molecules such as myelin-associated glycoprotein, L1, amphoterin, NCAM, PO, glycolipids.<sup>6</sup> It is possible that HNK-1 mimetic interactions with different molecules have different molecular and cellular consequences, both positive and negative, which are counterbalanced in a way to produce no effect in the parameters measured in this study. However, a more detailed survey of histological and functional parameters other than the ones used in this study could reveal effects that we have not been able to detect in the present study. It is noteworthy in this context that we found no adverse effects of the HNK-1 mimetic and testing of its efficacy in other injury paradigms is warranted.

### Therapeutic time window of the PSA glycomimetic

Based on our morphological evidence, we propose that enhanced plasticity underlies better functional outcome after PSA mimetic application in the acute phase of spinal cord injury. However, plasticity in both humans and laboratory animals is not restricted to the acute phase.<sup>44</sup> For example, using the same paradigm, we recently showed that spontaneous functional recovery and alterations in motoneuron connectivity and excitability occur to a high degree between the 6th and 12th week after injury.<sup>31</sup> Therefore, it appears surprising that we found no effect when the PSA mimetic was applied after the third postoperative week. One explanation is that, despite long-term progression, most of the spontaneous and crucial functional recovery in mice occurs within the first 3 weeks after spinal cord compression.<sup>18,22,31</sup> Thus, drug-induced positive functional effects at later stages of spinal cord regeneration might be difficult to measure. In addition, it is possible that a longer observation period after pump application is required to observe PSA effects 3 weeks after injury. This notion and the fact that spontaneous recovery in larger mammals and humans is slower than in the mouse, make us believe that application of PSA at a chronic stage in other injury paradigms or clinical settings could be effective.

In conclusion, our results warrant further experiments with PSA and HNK-1 mimetics, for example in larger laboratory animals, aiming to translate this approach into clinical practice. This notion is strongly encouraged by positive results achieved in an independent study using a different PSA mimetic and a different injury paradigm (dorsal hemisection) in mice.<sup>45</sup>

## MATERIALS AND METHODS

**Animals.** Three- to four-month-old female C57BL/6J mice were obtained from the central animal facility of the Universitätsklinikum Hamburg-Eppendorf. All experiments were conducted in accordance with the

German and European Community laws on the protection of experimental animals. The procedures used were approved by the responsible committee of the State of Hamburg. The animals were kept under standard laboratory conditions. Numbers of animals studied in different experimental groups and at different periods after surgery are given in the text and figures. All animal treatments, data acquisition and analyses were performed in a blinded fashion.

**Antibodies.** The following antibodies were used: goat anti-ChAT antibody (1:100; Chemicon, Hofheim, Germany), rabbit anti-tyrosine hydroxylase (1:800; Chemicon), and rabbit anti-vesicular glutamate transporter 1 (1:1,000; Synaptic Systems, Göttingen, Germany), and Cy3-conjugated goat anti-rabbit and donkey anti-goat antibodies (Jackson ImmunoResearch Laboratories, Dianova, Hamburg, Germany).

**Surgical procedures.** For surgery, mice were anesthetized by intraperitoneal injections of ketamin and xylazin (100 mg Ketanest, Parke-Davis/Pfizer, Karlsruhe, Germany, and 5 mg Rompun, Bayer, Leverkusen, Germany, per kg body weight). Laminectomy was performed at the T7–T9 level with mouse laminectomy forceps (Fine Science Tools, Heidelberg, Germany). A mouse spinal cord compression device was used to elicit compression injury.<sup>46</sup> Compression force (degree of closure of the forceps) and duration were controlled by an electromagnetic device: the spinal cord was maximally compressed (100%, according to the operational definition of Curtis *et al.*<sup>46</sup>) for 1 second by a time-controlled current flow through the electromagnetic device. Muscles and skin were then closed using 6-0 nylon stitches (Ethicon, Norderstedt, Germany). After the operation, mice were kept in a heated room (37°C) for several hours to prevent hypothermia and thereafter singly housed in a temperature-controlled (22°C) room with water and standard food provided *ad libitum*. During the postoperative period the bladders of the animals were manually voided twice daily.

**Osmotic pump implantation.** Alzet osmotic pumps (model 1002, 14 days infusion, Durect, Cupertino, CA) were filled with PBS alone or peptides (see below). Each pump was connected to a vinyl catheter (Durect). The distal tip of the catheter was stretched by hand upon fire to fit its diameter to the subdural space (<0.4 mm). For subdural insertion of the catheter, the lumbar vertebral column was exposed and a hole between vertebrae L4–L5 was made using a needle with a 0.4 mm outer diameter. Leakage of the cerebrospinal fluid was taken as proof for penetration of the dura. The catheter was then inserted into the hole and fixed to the surrounding tissue with a 6-0 filament (Ethicon). The pump was placed subcutaneously on the left side of the back over the thorax and the skin was closed with 6-0 nylon sutures. In pilot experiments, proper placement of the catheter in the subdural space was confirmed in four mice without spinal cord injury using magnetic resonance imaging (data not shown). After sacrifice of these animals 6 weeks after pump implantation, the appropriate catheter position was confirmed by macroscopic examination. During the 6-week observation period, no adverse effects of the pump implantation, such as infections, paralyzes, or aberrant behavior, were observed.

**Glycomimetic peptides.** The following peptides were infused: a linear PSA mimetic (sequence H-NHTHTDPYIYPID-OH,<sup>13</sup> a CON (sequence H-DSPLVPFIDFHPC-OH) and a cyclic HNK-1 mimetic (sequence c-(RTLPPFS)).<sup>15,16</sup> The linear peptide H-NHTHTDPYIYPID-OH was discovered in a phage display study as a functional mimetic of the PSA glycan.<sup>13</sup> The cyclic hexapeptide c-(RTLPPFS) is derived from the peptide sequence TFQLSTRTLPPFS discovered in phage display studies as a functional mimetic of the HNK-1 oligosaccharide.<sup>15,47</sup> This cyclic hexapeptide shows a higher binding affinity to the HNK-1 specific antibody 412 when compared to the original linear peptide and is also a functional mimetic of the HNK-1 oligosaccharide.<sup>15,16</sup>

**Infusion of human Fc fragment and western blot analysis.** The efficacy of the osmotic pumps was tested by infusion of the 50 kd human Fc fragment



(Jackson ImmunoResearch Laboratories). Two different concentrations were tested: 12.5 and 200 µg/ml. After 2 weeks of infusion, spinal cords were isolated and three 5 mm-long segments from each injured spinal cord were dissected: a segment at the thoracic level with the lesion scar in the center and two segments caudally, a lumbar and a sacral one. The samples were homogenized in ice-cold buffer containing 5 mmol/l Tris-HCl (pH 7.5), 0.32 mol/l sucrose, 1 mmol/l MgCl<sub>2</sub>, 1 mmol/l CaCl<sub>2</sub>, 1 mmol/l NaHCO<sub>3</sub>, and protease inhibitor cocktail (Roche Applied Science, Indianapolis, IN). Proteins denatured under nonreducing conditions were subjected to sodium dodecyl sulfate–polyacrylamide gel electrophoresis and transferred onto nitrocellulose membrane (Protran, Schleicher & Schuell, Dassel, Germany). Following pretreatment in 5% nonfat dry milk powder in 0.1% Tween-20 in PBS, pH 7.5 PBS, the membranes were incubated in 5% nonfat dry milk powder in PBS containing horseradish peroxidase-conjugated anti-human Fc (1:10,000; Sigma-Aldrich, St Louis, MO). After washing in 0.1% Tween-20 in PBS, immunoreactivity was detected by enhanced chemiluminescence (ECL kit; Amersham Biosciences, Piscataway, NJ) on Kodak Biomax X-ray film (Sigma-Aldrich) according to the manufacturer's instructions.

**Analysis of motor function.** The recovery of ground locomotion was evaluated using BMS.<sup>17</sup> In addition, we used a more complex and more objective assessment of locomotion, single-frame motion analysis.<sup>18</sup> This approach includes evaluation of four parameters in three different tests: beam walking (foot-stepping angle, rump-height index), voluntary movements without body weight support (extension–flexion ratio) and inclined ladder climbing (number of correct steps).<sup>18</sup> The foot-stepping angle is defined by a line parallel to the dorsal surface of the hindpaw and the horizontal line. The angle is measured with respect to the posterior aspect at the beginning of the stance phase. In intact mice, this phase is well defined and the angle is around 20°. After spinal cord injury and severe loss of locomotor abilities, the mice drag behind their hindlimbs with dorsal paw surfaces facing the beam surface. The angle is increased to >150°. The second parameter, the rump-height index, was estimated from the recordings used for measurements of the foot-stepping angle. The parameter is defined as height of the rump, *i.e.*, the vertical distance from the dorsal aspect of the animal's tail base to the beam, normalized to the thickness of the beam measured along the same vertical line. The third parameter, the limb extension–flexion ratio, was evaluated from video recordings of voluntary movements of the mice. An intact mouse, when held by its tail and allowed to grasp a pencil with its forepaws, tries to catch the object with its hindpaws and performs cycling flexion–extension movements with the hindlimbs. The extension–flexion ratio is a numerical estimate of the animal's ability to initiate and perform voluntary, nonweight bearing movements. Such movements require connectivity of the spinal cord to supraspinal motor control centers but, in the form evaluated here, no coordination or precision.

Assessment was performed before and at 1, 3, and 6 weeks after the injury. Values for the left and right extremities were averaged. RI were used as a measure of functional recovery at the individual animal level.<sup>18</sup> The RI is calculated (percentage) as follows:  $RI = [(X_{7+n} - X_7)/(X_0 - X_7)] \times 100$ , where  $X_0$ ,  $X_7$ , and  $X_{7+n}$  are values before operation, 7 days after injury, and a time point  $n$  days after the spinal cord injury, respectively. In simpler terms, this measure estimates gain of function ( $X_{7+n} - X_7$ ) as a fraction of the functional loss ( $X_0 - X_7$ ) induced by the operation. It may attain 0 or negative values if no improvement or additional impairment occurs during the observation period. The index cannot be calculated only if the operation causes no change in the value ( $X_0 - X_7 = 0$ ). The recovery index is a meaningful and comprehensive parameter allowing better comparisons within one investigation and between results of different laboratories. Calculation of RI is absolutely necessary if a parameter is prone to variability as a result of individual animal variability in body constitution and behavioral traits. An example is the rump-height index defined above. The index values are influenced not only by functional impairment but also by the animal's body size and the beam thickness. Overall RI were calculated, on an individual animal basis, as means of RI for the four

parameters: BMS, foot-stepping angle, rump-height index and extension/flexion ratio. The overall index is an estimate of the general condition of the treated animals based on individual objective measures. It is taken as a “clinical score” for individual mice similar to the BMS, which is based on assessment of different aspects of locomotion.

**Tissue fixation and sectioning.** Mice were anaesthetized with a 16% solution of sodium pentobarbital (Narcoren, Merial, Hallbergmoos, Germany, 5 µl/g body weight). The animals were transcardially perfused with fixative consisting of 4% formaldehyde and 0.1% CaCl<sub>2</sub> in 0.1 mol/l cacodylate buffer, pH 7.3, for 15 minutes at room temperature (RT). Following perfusion, the spinal cords were left *in situ* for 2 hours at RT, after which they were dissected out and postfixed overnight (18–22 hours) at 4°C in the same solution used for perfusion. Tissue was then immersed into a 15% sucrose solution in 0.1 mol/l cacodylate buffer, pH 7.3, for 2 days at 4°C, embedded in Tissue Tek (Sakura Finetek, Zoeterwoude, NL), and frozen by a 2 minute immersion into 2-methyl-butane (isopentane) precooled to –80°C. Serial transverse or parasagittal sections were cut in a cryostat (Leica CM3050, Leica Instruments, Nussloch, Germany). Sections, 25 µm-thick, were collected on SuperFrost Plus glass slides (Roth, Karlsruhe, Germany). Sampling of sections was always done in a standard sequence so that six sections 250 µm apart were present on each slide.

**Immunohistochemistry.** Procedures for immunohistochemistry have been described.<sup>48</sup> Water bath antigen de-masking was performed in 0.01 mol/l sodium citrate solution, pH 9.0, for 30 minutes at 80°C for all antigens. Nonspecific binding was blocked using 5% normal serum from the species in which the secondary antibody was produced, dissolved in PBS and supplemented with 0.2% Triton X-100, 0.02% sodium azide for 1 hour at RT. Incubation with the primary antibody (anti-ChAT, anti-VGLUT1 or anti-tyrosine hydroxylase), diluted in PBS containing 0.5% lambda-carrageenan (Sigma) and 0.02% sodium azide, was carried out for 3 days at 4°C. After washing in PBS (3 × 15 minutes at RT), the appropriate secondary antibody, diluted 1:200 in PBS-carrageenan solution, was applied for 2 hours at RT. After a subsequent wash in PBS, cell nuclei were stained for 10 minutes at RT with bis-benzimide solution (Hoechst 33258 dye, 5 µg/ml in PBS, Sigma). Finally, the sections were washed again, mounted in anti-quenching medium (Fluoromount G; Southern Biotechnology Associates, Biozol, Eching, Germany) and stored in the dark at 4°C. Photographic documentation was made on an LSM 510 confocal microscope (Zeiss, Oberkochen, Germany) or an Axiophot two microscope equipped with a digital camera AxioCam HRC and AxioVision software (Zeiss). The images were processed using Adobe Photoshop 7.0 software (Adobe Systems, San Jose, CA).

**Quantification of motoneuron numbers in the lumbar spinal cord.** Motoneuron counts were performed using the optical dissector method on an Axioskop microscope (Zeiss) equipped with a motorized stage and NeuroLucida software-controlled computer system (MicroBrightField, Colchester, VT).<sup>48,49</sup> For each animal, eight equidistant (250 µm apart) transverse sections from the lumbar spinal cord stained for ChAT and nuclei were analyzed. Using the nuclear staining, the ventral horn areas on both sides of each section were outlined with the cursor of the software under low-power magnification (×10 objective). All ChAT-positive motoneurons in the ventral horn motor nuclei (Rexed laminae VIII and IX) with nuclei appearing in focus within 2–12 µm from the top of the section were counted using a Plan-Neofluar ×40/0.75 objective. Cell densities were calculated by dividing the cell number by the reference volume (ventral horn area × 10 µm) and averaged per animal.

**Motoneuron soma size and quantification of perisomatic terminals.** Estimations of motoneuron soma areas and perisomatic terminals were performed as described.<sup>18</sup> Transverse spinal cord sections stained for ChAT or VGLUT1 were examined under a fluorescence microscope to select sections that contained motoneuron cell bodies for a distance of at

least 500  $\mu\text{m}$  distal from the lesion scar. Stacks of 1  $\mu\text{m}$ -thick images were obtained on the LSM 510 confocal microscope using a  $63 \times 1.5$  oil immersion objective and digital resolution of  $512 \times 512$  pixels. One image (optical slice) per cell at the level of the largest cell body cross-sectional area was used to measure soma area, perimeter and number of perisomatic terminals. Areas and perimeters were measured using the Image Tool 2.0 software program (University of Texas, San Antonio, TX). Density of ChAT<sup>+</sup> terminals was calculated as number of perisomatic terminals per unit length of the cell surface. For VGLUT1<sup>+</sup> terminals, densities per area in the Clarke's column, Lamina VII and ventral horns were measured using the Image J software (<http://rsbweb.nih.gov/ij/download.html>).

**Estimation of lesion scar volume and myelin volume.** Spaced serial 25  $\mu\text{m}$ -thick transverse sections 250  $\mu\text{m}$  apart were stained with Cresyl Violet/luxol fast blue and used for estimations of the scar volume and myelin volume using the Cavalieri principle. Area measurements required for volume estimation were done directly under the microscope using the NeuroLucida software (MicroBrightField).

**Analyses of axonal myelination.** Spinal cords were dissected from animals fixed by perfusion with formaldehyde (see above). From each specimen, 0.6 cm-long segments were cut from the lumbar and thoracic part of the spinal cord at distances of  $\sim 5$  mm distal and proximal to the center of the lesion, respectively. Tissue was postfixed in 1% osmium tetroxide in 0.1 mol/l sodium cacodylate buffer, pH 7.3, for 1 hour at RT, dehydrated and embedded in resin according to standard protocols. Transverse 1  $\mu\text{m}$ -thick sections were cut (Ultramicrotome, Leica) and stained with 1% toluidine blue/ 1% borax in distilled water. Axonal and nerve fiber diameters in the ventral funiculus were measured in a random sample using the  $\times 100$  oil objective of the Axioskop microscope (Zeiss) and the NeuroLucida software (MicroBrightField). For sampling, a grid with line spacing of 30  $\mu\text{m}$  was projected into the microscope visual field using the NeuroLucida software (MicroBrightField). Selection of the reference point (zero coordinates) of the grid was random. For all myelinated axons crossed by or attaching to the vertical grid lines through the sections, mean orthogonal diameters of the axon (inside the myelin sheath) and of the nerve fiber (including the myelin sheath) were measured. The mean orthogonal diameter is calculated as a mean of the line connecting the two most distal points of the profile (longest axis) and the line passing through the middle of the longest axis at right angle.<sup>50</sup> The degree of myelination was estimated by the ratio of axon-to-fiber diameter (g-ratio).

**Statistical analysis.** All numerical data are presented as group mean values with SEM. Parametric or nonparametric tests were used for comparisons, as indicated in the text and figure legends. Analyses were performed using the SYSTAT 9 software package (SPSS, Chicago, IL). The threshold value for acceptance of differences was 5%.

## ACKNOWLEDGMENTS

We are grateful to Emanuela Szpotowicz for excellent technical assistance. This work was supported by the New Jersey commission for Spinal Cord Research. Melitta Schachner is New Jersey Professor for Spinal Cord Research.

## REFERENCES

- Ramón y Cajal, S (1928). *Degeneration and regeneration of the nervous system*. Oxford University Press: London, New York.
- Schwab, ME (2002). Repairing the injured spinal cord. *Science* **295**: 1029–1031.
- Fawcett, JW (2006). Overcoming inhibition in the damaged spinal cord. *J Neurotrauma* **23**: 371–383.
- Loers, G and Schachner, M (2007). Recognition molecules and neural repair. *J Neurochem* **101**: 865–882.
- Rossi, F, Buffo, A and Strata, P (2001). Regulation of intrinsic regenerative properties and axonal plasticity in cerebellar Purkinje cells. *Restor Neurol Neurosci* **19**: 85–94.
- Kleene, R and Schachner, M (2004). Glycans and neural cell interactions. *Nat Rev Neurosci* **5**: 195–208.
- Rutishauser, U and Landmesser, L (1996). Polysialic acid in the vertebrate nervous system: a promoter of plasticity in cell-cell interactions. *Trends Neurosci* **19**: 422–427.
- Rutishauser, U (2008). Polysialic acid in the plasticity of the developing and adult vertebrate nervous system. *Nat Rev Neurosci* **9**: 26–35.
- Durbec, P and Cremer, H (2001). Revisiting the function of PSA-NCAM in the nervous system. *Mol Neurobiol* **24**: 53–64.
- El Maarouf, A, Petridis, AK and Rutishauser, U (2006). Use of polysialic acid in repair of the central nervous system. *Proc Natl Acad Sci USA* **103**: 16989–16994.
- Papastefanaki, F, Chen, J, Lavdas, AA, Thomaidou, D, Schachner, M and Matsas, R (2007). Grafts of Schwann cells engineered to express PSA-NCAM promote functional recovery after spinal cord injury. *Brain* **130**(Pt 8): 2159–2174.
- Zhang, Y, Zhang, X, Wu, D, Verhaagen, J, Richardson, PM, Yeh, J *et al.* (2007). Lentiviral-mediated expression of polysialic acid in spinal cord and conditioning lesion promote regeneration of sensory axons into spinal cord. *Mol Ther* **15**: 1796–1804.
- Mehanna, A, Mishra, B, Kurschat, N, Schulze, C, Bian, S, Loers, G *et al.* (2009). Polysialic acid glycomimetics promote myelination and functional recovery after peripheral nerve injury in mice. *Brain* **132**(Pt 6): 1449–1462.
- Miura, R, Asperger, A, Ethell, IM, Hagihara, K, Schnaar, RL, Ruoslahti, E *et al.* (1999). The proteoglycan lectin domain binds sulfated cell surface glycolipids and promotes cell adhesion. *J Biol Chem* **274**: 11431–11438.
- Bächle, D, Loers, G, Guthöhrlein, EW, Schachner, M and Sewald, N (2006). Glycomimetic cyclic peptides stimulate neurite outgrowth. *Angew Chem Int Ed Engl* **45**: 6582–6585.
- Simova, O, Irintchev, A, Mehanna, A, Liu, J, Dihné, M, Bächle, D *et al.* (2006). Carbohydrate mimics promote functional recovery after peripheral nerve repair. *Ann Neurol* **60**: 430–437.
- Basso, DM, Fisher, LC, Anderson, AJ, Jakeman, LB, McTigue, DM and Popovich, PG (2006). Basso Mouse Scale for locomotion detects differences in recovery after spinal cord injury in five common mouse strains. *J Neurotrauma* **23**: 635–659.
- Apostolova, I, Irintchev, A and Schachner, M (2006). Tenascin-R restricts posttraumatic remodeling of motoneuron innervation and functional recovery after spinal cord injury in adult mice. *J Neurosci* **26**: 7849–7859.
- Kloos, AD, Fisher, LC, Detloff, MR, Hassenzahl, DL and Basso, DM (2005). Stepwise motor and all-or-none sensory recovery is associated with nonlinear sparing after incremental spinal cord injury in rats. *Exp Neurol* **191**: 251–265.
- Crutcher, KA and Bingham, WG Jr (1978). Descending monoaminergic pathways in the primate spinal cord. *Am J Anat* **153**: 159–164.
- Heckman, CJ, Lee, RH and Brownstone, RM (2003). Hyperexcitable dendrites in motoneurons and their neuromodulatory control during motor behavior. *Trends Neurosci* **26**: 688–695.
- Jakovcevski, I, Wu, J, Karl, N, Leshchyns'ka, I, Sytnyk, V, Chen, J *et al.* (2007). Glial scar expression of CHL1, the close homolog of the adhesion molecule L1, limits recovery after spinal cord injury. *J Neurosci* **27**: 7222–7233.
- Davidoff, MS and Irintchev, AP (1986). Acetylcholinesterase activity and type C synapses in the hypoglossal, facial and spinal-cord motor nuclei of rats. An electron-microscope study. *Histochemistry* **84**: 515–524.
- Hellström, J, Oliveira, AL, Meister, B and Cullheim, S (2003). Large cholinergic nerve terminals on subsets of motoneurons and their relation to muscarinic receptor type 2. *J Comp Neurol* **460**: 476–486.
- Miles, GB, Hartley, R, Todd, AJ and Brownstone, RM (2007). Spinal cholinergic interneurons regulate the excitability of motoneurons during locomotion. *Proc Natl Acad Sci USA* **104**: 2448–2453.
- Dietz, V (2002). Proprioception and locomotor disorders. *Nat Rev Neurosci* **3**: 781–790.
- Lavrov, I, Courtine, G, Dy, CJ, van den Brand, R, Fong, AJ, Gerasimenko, Y *et al.* (2008). Facilitation of stepping with epidural stimulation in spinal rats: role of sensory input. *J Neurosci* **28**: 7774–7780.
- Brumovsky, P, Watanabe, M and Hökfelt, T (2007). Expression of the vesicular glutamate transporters-1 and -2 in adult mouse dorsal root ganglia and spinal cord and their regulation by nerve injury. *Neuroscience* **147**: 469–490.
- Charles, P, Hernandez, MP, Stankoff, B, Aigrot, MS, Colin, C, Rougon, G *et al.* (2000). Negative regulation of central nervous system myelination by polysialylated-neural cell adhesion molecule. *Proc Natl Acad Sci USA* **97**: 7585–7590.
- Jakovcevski, I, Mo, Z and Zecevic, N (2007). Down-regulation of the axonal polysialic acid-neural cell adhesion molecule expression coincides with the onset of myelination in the human fetal forebrain. *Neuroscience* **149**: 328–337.
- Lee, HJ, Jakovcevski, I, Radonjic, N, Hoelters, L, Schachner, M and Irintchev, A (2009). Better functional outcome of compression spinal cord injury in mice is associated with enhanced H-reflex responses. *Exp Neurol* **216**: 365–374.
- Edgerton, VR, Tillakaratne, NJ, Bigbee, AJ, de Leon, RD and Roy, RR (2004). Plasticity of the spinal neural circuitry after injury. *Annu Rev Neurosci* **27**: 145–167.
- Fouad, K and Pearson, K (2004). Restoring walking after spinal cord injury. *Prog Neurobiol* **73**: 107–126.
- Hallett, M (2007). Volitional control of movement: the physiology of free will. *Clin Neurophysiol* **118**: 1179–1192.
- Kloosterman, MG, Snoek, GJ and Jannink, MJ (2009). Systematic review of the effects of exercise therapy on the upper extremity of patients with spinal-cord injury. *Spinal Cord* **47**: 196–203.
- Frigon, A and Rossignol, S (2006). Functional plasticity following spinal cord lesions. *Prog Brain Res* **157**: 231–260.
- Bock, E, Edvardsen, K, Gibson, A, Linnemann, D, Lyles, JM and Nybroe, O (1987). Characterization of soluble forms of NCAM. *FEBS Lett* **225**: 33–36.
- Olsen, M, Krog, L, Edvardsen, K, Skovgaard, LT and Bock, E (1993). Intact transmembrane isoforms of the neural cell adhesion molecule are released from the plasma membrane. *Biochem J* **295**(Pt 3): 833–840.
- Curreli, S, Arany, Z, Gerardy-Schahn, R, Mann, D and Stamatou, NM (2007). Polysialylated neuropilin-2 is expressed on the surface of human dendritic cells and modulates dendritic cell-T lymphocyte interactions. *J Biol Chem* **282**: 30346–30356.
- Doherty, P, Fruns, M, Seaton, P, Dickson, G, Barton, CH, Sears, TA *et al.* (1990). A threshold effect of the major isoforms of NCAM on neurite outgrowth. *Nature* **343**: 464–466.

41. Becker, CG, Artola, A, Gerardy-Schahn, R, Becker, T, Welzl, H and Schachner, M (1996). The polysialic acid modification of the neural cell adhesion molecule is involved in spatial learning and hippocampal long-term potentiation. *J Neurosci Res* **45**: 143–152.
42. Dityatev, A, Dityateva, G, Sytnyk, V, Dellling, M, Toni, N, Nikonenko, I *et al.* (2004). Polysialylated neural cell adhesion molecule promotes remodeling and formation of hippocampal synapses. *J Neurosci* **24**: 9372–9382.
43. Dityatev, A and Schachner, M (2006). The extracellular matrix and synapses. *Cell Tissue Res* **326**: 647–654.
44. Little, JW, Ditunno, JF Jr, Stiens, SA and Harris, RM (1999). Incomplete spinal cord injury: neuronal mechanisms of motor recovery and hyperreflexia. *Arch Phys Med Rehabil* **80**: 587–599.
45. Marino, P, Norreel, JC, Schachner, M, Rougon, G and Amoureux, MC (2009). A polysialic acid mimetic peptide promotes functional recovery in a mouse model of spinal cord injury. *Exp Neurol* **219**: 163–174.
46. Curtis, R, Green, D, Lindsay, RM and Wilkin, GP (1993). Up-regulation of GAP-43 and growth of axons in rat spinal cord after compression injury. *J Neurocytol* **22**: 51–64.
47. Simon-Haldi, M, Mantei, N, Franke, J, Voshol, H and Schachner, M (2002). Identification of a peptide mimic of the L2/HNK-1 carbohydrate epitope. *J Neurochem* **83**: 1380–1388.
48. Irintchev, A, Rollenhagen, A, Troncoso, E, Kiss, JZ and Schachner, M (2005). Structural and functional aberrations in the cerebral cortex of tenascin-C deficient mice. *Cereb Cortex* **15**: 950–962.
49. Jakovcevski, I, Siering, J, Hargus, G, Karl, N, Hoelters, L, Djogo, N *et al.* (2009). Close homologue of adhesion molecule L1 promotes survival of Purkinje and granule cells and granule cell migration during murine cerebellar development. *J Comp Neurol* **513**: 496–510.
50. Irintchev, A, Draguhn, A and Wernig, A (1990). Reinnervation and recovery of mouse soleus muscle after long-term denervation. *Neuroscience* **39**: 231–243.